Oligothiophene-Bridged Bis(arylene ethynylene) Small Molecules for Solution-Processible Organic Solar Cells with High Open-Circuit Voltage

ARTICLE *in* CHEMISTRY - AN ASIAN JOURNAL · AUGUST 2013

Impact Factor: 4.59 · DOI: 10.1002/asia.201300244 · Source: PubMed

11 AUTHORS, INCLUDING:

Cheuk-Lam Ho

76 PUBLICATIONS **3,143** CITATIONS

SEE PROFILE

Feng-Rong Dai

Chinese Academy of Sciences

29 PUBLICATIONS **351** CITATIONS

SEE PROFILE

Jinhua Li

Hubei University

36 PUBLICATIONS **903** CITATIONS

SEE PROFILE

Feng Yan

The Hong Kong Polytechnic University

90 PUBLICATIONS **2,289** CITATIONS

SEE PROFILE

CHEMISTRY
AN ASIAN JOURNAL
ACES
FULL PAPER

DOI: 10.1002/asia.201300244

Oligothiophene-Bridged Bis(arylene ethynylene) Small Molecules for Solution-Processible Organic Solar Cells with High Open-Circuit Voltage

Qian Liu,[a] Hongmei Zhan,[a] Cheuk-Lam Ho,*[a] Feng-Rong Dai,[a] Yingying Fu,[b] Zhiyuan Xie,*[b] Lixiang Wang,[b] Jin-Hua Li,[c] Feng Yan,*[c] Shu-Ping Huang,[d] and Wai-Yeung Wong*[a]

Abstract: A new series of conjugated oligothiophene-bridged bis(arylene ethynylene) small molecules have been designed, synthesized, and characterized by photophysical, electrochemical and computational methods. These compounds were found to have optimal LUMO levels that ensure effective charge transfer from these compounds to [6,6]-phenyl-C_{71}-butyric acid methyl ester ($PC_{70}BM$). They were utilized as good electron-donor materials that can be blended with electron-acceptor $PC_{70}BM$ in the fabrication of solution-processed molecular bulk heterojunction (BHJ) solar cells. All of these BHJ devices showed very high open-circuit voltage (V_{oc}) of 0.90–0.97 V, and the best power conversion efficiency achieved was 3.68%. The high V_{oc} is consistent with the deeper low-lying HOMO level and is relatively insensitive to the donor : acceptor blend ratio. The spin-coated thin films of these small molecules showed p-channel field-effect charge transport with the hole mobilities of up to 2.04×10^{-4} $cm^2 V^{-1} s^{-1}$. These compounds illuminate the potential of solution-processible small-molecular aryl acetylide compounds for efficient power generation in photovoltaic implementation.

Keywords: arylene ethynylenes · donor–acceptor systems · molecular electronics · organic solar cells

Introduction

With the recent increase in awareness of environmental protection, topics on renewable energy sources are getting more important in the scientific community.[1] Research on organic solar cells (OSCs) using conjugated molecular materials has attracted increasing attention in recent years because these organic devices possess several advantages over mainstream inorganic-based solar cells, such as significantly reduced fabrication cost and consumption of materials, flexible substrates and light weight of finished solar cells, and great promise in energy-generating applications.[2] Much work on designing new materials,[3] device structures,[4] and processing techniques[5] has been carried out to improve the power conversion efficiency (PCE) of such devices. In recent years, many researchers have made great progress in the development of bulk heterojunction (BHJ) solar cell since their inception in 1995.[6] Most of the BHJ solar cells comprise a donor–acceptor (D–A) system of conjugated polymers or small molecules as photoactive materials (as D unit) and fullerene derivatives (as A unit). OSCs based on p-type conjugated polymers have shown PCEs of up to 8.3% in 2011[7] and 9.2% in 2012.[8] Although the PCEs of OSCs derived from small molecules are still below those of polymer-based devices, solution-processible small-molecule OSCs have been actively studied.[6a,9–11] Small molecules are easy to synthesize in high purity and possess well-defined structures, which are in contrast to polymeric systems that intrinsically display large structural variations in the molecular weight, polydispersity, and regioregularity. In addition, small molecules typically show higher charge-carrier mobilities.[12] An increasing number of publications on BHJ solar cells based on small molecules has recently appeared, and the PCE values of these BHJ devices fabricated by vacuum

[a] Q. Liu,[+] Dr. H.-M. Zhan,[+] Dr. C.-L. Ho, Dr. F.-R. Dai, Prof. W.-Y. Wong
Institute of Molecular Functional Materials
Department of Chemistry and Institute of Advanced Materials
Hong Kong Baptist University
Waterloo Road, Kowloon Tong, Hong Kong (P.R. China)
E-mail: rwywong@hkbu.edu.hk
clamho@hkbu.edu.hk

[b] Y. Fu, Prof. Z.-Y. Xie, Prof. L.-X. Wang
State Key Laboratory of Polymer Physics and Chemistry
Changchun Institute of Applied Chemistry
Chinese Academy of Sciences
Changchun 130022 (P.R. China)
E-mail: xiezy_n@ciac.jl.cn

[c] J.-H. Li, Prof. F. Yan
Department of Applied Physics
The Hong Kong Polytechnic University
Hung Hom, Hong Kong (P.R. China)
E-mail: feng.yan@inet.polyu.edu.hk

[d] Dr. S.-P. Huang
Institute for Materials Chemistry and Engineering and International Research Center for Molecular Systems
Kyushu University
Fukuoka 819-0395 (Japan)

[+] These authors contributed equally to this work.

deposition or solution processing have evolved from <1% to a recent value of over 8%.[6a,11b,13,14]

The donor–acceptor–donor (D–A–D) system is the basic structural framework for most organic photoactive materials due to its effective photoinduced intramolecular charge-transfer (ICT) transition. While the introduction of a triple bond into the molecular linker unit of conjugated organic molecules has been less commonly explored in the molecular design of photovoltaic materials, it can be an alternative approach for improving the OSC performance of the resulting compound.[15] The linker contributes not only to the light absorption process but also to the charge transfer, in which it serves as a transport channel. Adding a triple bond unit should also promote the absorption of light over a wider wavelength region, thus red-shifting the absorption maximum and offering the ability to decrease the energy level of the highest occupied molecular orbital (HOMO), which is directly correlated to the open-circuit voltage (V_{oc}) of the photovoltaic devices.[16] Moreover, the availability of efficient synthetic protocols mentioned above allows the easy variation of specific structural features of the molecules. With this background in mind, we report herein the synthesis and characterization of a new series of oligothiophene-linked bis(arylene ethynylene) compounds with a D–A–spacer–A–D building motif for small-molecule BHJ solar cells in which 2,1,3-benzothiadiazole acts as the acceptor unit and triarylamine as the donor unit. The two hexyl side chains on the thiophene π bridge are used to improve the solubility and film-forming properties. Different chain lengths of the oligothiophene component were employed to fine-tune the ICT strength of the D–A component. The synthetic procedures of these compounds are simple, and the product yields are good. All of these products are easy to purify by flash column chromatography on silica gel using the appropriate eluent. These compounds have been applied successfully in BHJ devices, and the corresponding optical, electronic, and photovoltaic properties have been carefully studied; their structure–photovoltaic property relationships with different spacers are also presented.

Abstract in Chinese:

一系列新型的共轭桥联的双(芳基乙炔)低聚噻吩小分子已被设计合成，并通过光物理，电化学和计算的方法对其进行了表征。这些新型的小分子具有最佳的分子最低未占有轨道(LUMO)能级，确保它们的有效电荷能够转移至[6,6]-苯基-C_{71}-酸甲基酯($PC_{70}BM$)。它们是良好的电子给体材料，可以与电子受体 $PC_{70}BM$ 进行掺杂，制造溶液可处理分子型体异质结(BHJ)太阳能电池。所有这些 BHJ 器件都具有非常高的开路电压，达到了 0.90–0.97 V，其中最好的能量转换效率高达 3.68%。高的开路电压与更深的低洼分子最高已占有轨道(HOMO)能级，以及对给体：受体混合比例相对不敏感是一致的。这些小分子的旋涂薄膜具有 p-沟道场效应，它的电荷传输空穴迁移率达到了 2.04×10^{-4} cm^2 V^{-1} s^{-1}。这些新型的小分子具有很好的光伏应用，为溶液可加工小分子芳炔化合物的高效光伏发电提供了可行性方案。

Results and Discussion

Synthesis and Characterization

The key compound **L1** was prepared according to the reported procedures.[17] The synthetic routes to the tetraacetylenic control molecule **1** and the oligothiophene-bridged bis(arylene ethynylene) compounds **2–4** are illustrated in Scheme 1. In the presence of a catalytic amount of [Pd(PPh_3)$_4$] and CuI, **1** was obtained in a very high yield (97%) by the self-coupling reaction of the monoethynyl ligand **L1**. Compounds **2–4** were prepared by the Sonogashira coupling reaction between diiodo-substituted oligothiophenes and **L1** with a mixture of $Pd(OAc)_2$, CuI, and PPh_3 as the catalyst (Scheme 1).[18] All of these well-defined small molecules can be easily purified by chromatography on silica gel and are soluble in common organic solvents, such as CH_2Cl_2, $CHCl_3$, THF, and toluene. They were fully characterized by common spectroscopic techniques, including IR, ^{1}H NMR, and ^{13}C NMR spectroscopy and MALDI-TOF mass spectrometry. The IR spectra of these compounds showed characteristic ν(C≡C) bands at 2057–2124 cm^{-1}, and the absence of terminal acetylenic C≡C–H stretching vibrations in **1–4** is consistent with the formation of the coupling products. In each case, the MALDI-TOF mass spectrum gave the respective molecular ion peak $[M]^+$. The symmetrical patterns of the ^{1}H NMR spectra of **1–4** agree with the proposed structures, showing the expected features with correct integration ratios. There are also two distinct ^{13}C resonance peaks due to the presence of two acetylide units in these symmetric molecules.

Photophysical and Electrochemical Properties

The photophysical properties of the newly synthesized compounds **1–4** were investigated by UV/Vis and photoluminescence (PL) spectroscopy in CH_2Cl_2 at 293 K and compared with those of the monoethynyl ligand **L1**. The photophysical data are collected in Table 1. As illustrated in Figure 1, compounds **1–4** showed two major strong absorption bands and a shoulder peak covering a wide range of the visible region between 270 and 650 nm. The absorption bands at the short wavelengths centered at 308–330 nm are ascribed to the π→π* transitions of the arylene ethynylene segment. The low-energy absorption bands centered at 483–514 nm can be assigned to the intramolecular charge-transfer (ICT) transition

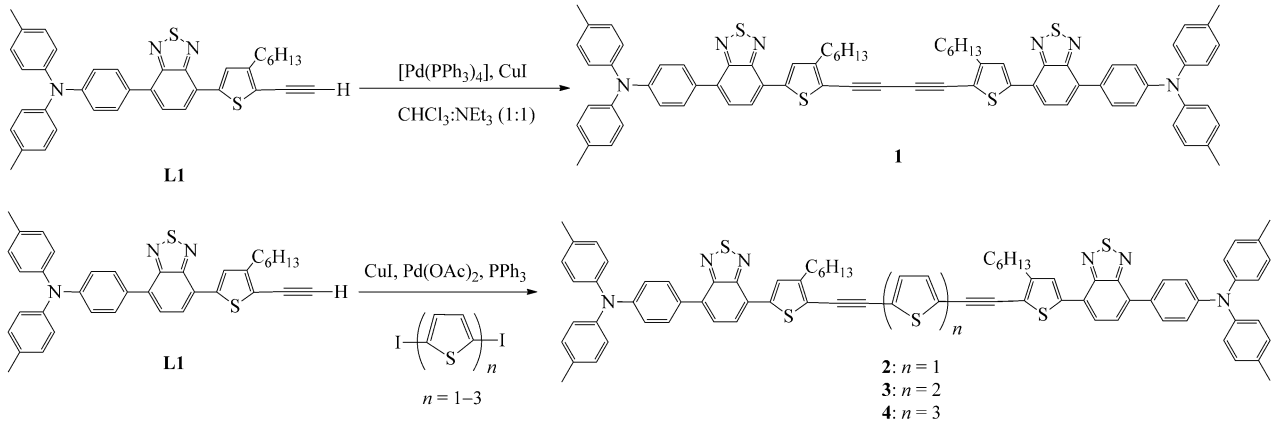

Scheme 1. Synthetic routes to new oligothiophene-bridged bis(arylene ethynylene) compounds.

Table 1. Photophysical data for compounds **L1** and **1–4** in CH_2Cl_2 at 293 K.

	Absorption		Emission		
	λ_{abs} [nm] (ε [10^4 M^{-1}cm^{-1}])[a]	onset λ_{abs} [nm]	λ_{em} [nm]	Φ_F [%][b]	τ_F [ns]
1	307 (9.09), 363 sh (6.32), 514 (8.90)	596	672	10.49	4.05
2	311 (6.57), 387 sh (4.06), 505 (7.24)	599	670	11.02	4.53
3	313 (4.45), 439 sh (3.32), 507 (5.68)	601	671	10.55	4.64
4	315 (5.23), 461 sh (5.14), 508 (6.79)	604	668	10.18	5.24
L1	330 (2.39), 483 (1.29)	567	668	9.56	–

[a] sh = shoulder peak. [b] Quantum yields were measured with an excitation wavelength of 488 nm using rhodamine 6G in water as the reference ($\Phi_F = 0.95$).[20]

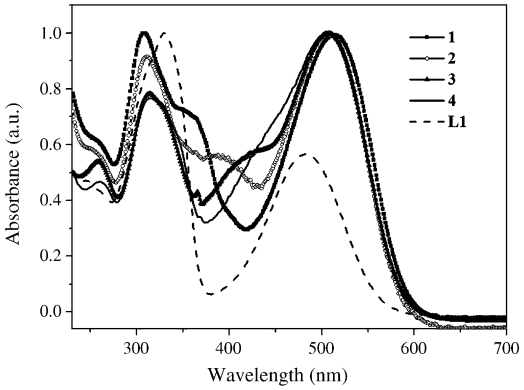

Figure 1. Absorption spectra of **L1** and **1–4** in CH_2Cl_2 at 293 K.

between the triarylamine or thiophene electron-donating groups and the benzothiadiazole electron-accepting unit in this D–A–spacer–A–D molecular architecture. A red shift of the low-energy absorption in **1–4** by 23–31 nm compared to the free ligand **L1** ($\lambda_{max} = 483$ nm) is expected due to the increased electronic conjugation length as well as the increased ICT strength within the molecules. The amount of the absorbed light depends not only on the cut-off wavelength of the absorption but also on how intense the absorption is. Therefore, the design of the low-bandgap molecules for photovoltaic applications should consider not only lowering the gap but also increasing the absorption coefficient of the material. Here, the absorption intensities of **1–4** are enhanced significantly as compared to **L1**, thus giving rise to higher molar absorption coefficients for **1–4**. This phenomenon is similarly ascribed to the strong intramolecular D–A interactions in these extended π-conjugated molecules.[17,19] The absorption profiles for **1–4** are virtually unaffected by the addition of a central linker unit or an increase of the number of thiophene rings in the linker, but these features slightly affect the extent of π delocalization along the molecular backbone. The low-energy absorption maxima of **1–4** are located at 505–514 nm with molar absorptivities of 5.68–8.90×10^4 M^{-1}cm^{-1}. As expected, compound **4**, with the longest absorption edge (Figure 1), displays the lowest optical band gaps ($E_g = 2.05$ V), because it also has the strongest ICT interaction.

We also performed photoluminescence (PL) studies on **L1** and **1–4** in CH_2Cl_2 at 293 K (Figure 2). Compound **L1** exhibited a red emission peak at 668 nm, while **1–4** showed the PL maxima within the narrow range of 668–672 nm with respective emission lifetimes of 4.05, 4.53, 4.64, and 5.24 ns, indicative of their fluorescent nature. The broad and structureless patterns of their emission spectra suggest that the origins of their emissive excited states are ICT in nature.

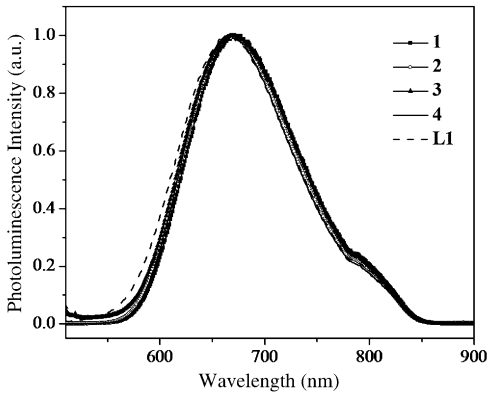

Figure 2. Photoluminescence spectra of **L1** and **1–4** in CH_2Cl_2 at 293 K.

The charge-transfer nature of the transition was also supported by the solvent-dependent emission spectra of our compounds in solvents of different polarities (Table 2). For example, compound **1** exhibited a marked positive solvatochromism with a red shift of the emission maximum of approximately 54 nm from toluene (λ_{em}=618 nm) to CH_2Cl_2 (λ_{em}=672 nm), which suggests a less polar excited state (Figure 3). A similar bathochromic shift of 53 nm (or 49 nm) was observed for **2** (or **4**) upon changing the solvent from toluene to CH_2Cl_2.

Table 2. Solvatochromic effect of the PL data for selected compounds.[a]

	Toluene	$CHCl_3$	CH_2Cl_2
1	618	653	672
2	617	652	670
4	619	653	668

[a] Onset λ_{abs} [nm].

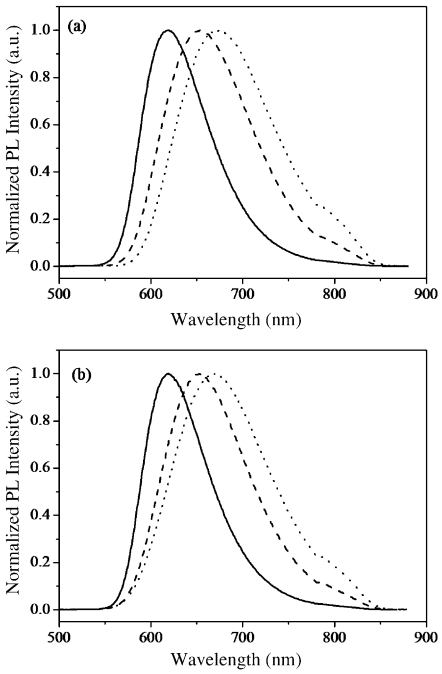

Figure 3. Positive solvatochromism of the PL spectra for a) **1** and b) **2**. —— toluene, – – – $CHCl_3$, ····· CH_2Cl_2.

The electronic levels of an organic semiconductor are crucial for governing the overall photovoltaic performance.[21] To evaluate the oxidation (E_{ox}) and reduction potentials (E_{red}) of these conjugated molecules, cyclic voltammetry (CV) was performed on their thin films on glassy carbon electrode measured in 0.1 mol L^{-1} $[Bu_4N][PF_6]$ in acetonitrile with a Pt wire counter electrode and a Ag/AgCl reference electrode under N_2 atmosphere at a scan rate of 50 mV s^{-1}. The HOMO and lowest unoccupied molecular orbital (LUMO) levels are calculated from the onset potentials of oxidation and reduction and by assuming the energy level of ferrocene/ferrocenium (Fc/Fc^+) to be −4.8 eV below the vacuum level. The formal potential of Fc/Fc^+ was measured as 0.07 V versus Ag/AgCl, which has an absolute energy level of −4.73 eV relative to the vacuum level for calibration.[17,19] The four new compounds have similar onset E_{ox} and E_{red} values. The HOMO and LUMO energy levels were determined by using the following equations: HOMO = $-(E_{ox}+4.73)$ eV and LUMO = $-(E_{red}+4.73)$ eV. The results are summarized in Table 3 and the CV curves are shown in Figure 4. As compared with the HOMO (−5.87 eV) and LUMO (−3.91 eV) energy levels for [6,6]-phenyl-C_{71}-butyric acid methyl ester ($PC_{70}BM$),[22] our compounds are suitable candidates as donor materials in OSCs when blended with $PC_{70}BM$ acceptor since **1**–**4** have their LUMO levels at around −3.6 eV, which are higher than the $PC_{70}BM$ level, making photoinduced ICT and charge separation possible at the interface between the D and A units (see below). In addition, for effective charge separation and transfer from D to A to take place, the LUMO level of the donor needs to be 0.3 to 0.5 eV higher than the LUMO of the acceptor,[23] but this energy difference is much higher than those for most of the D groups currently used in OSCs. The deeper HOMO level of our donor compounds is beneficial to the higher V_{oc} of the OSCs, because the V_{oc} is generally proportional to the difference between the LUMO level of the acceptor and the HOMO level of the donor.[24] The LUMO values of our compounds are also favorable for obtaining the optimal V_{oc} in the device.[16,25] The difference between the oxidation and reduction potentials gives access to the electrochemical band gap ($E_{g,ec}$). The $E_{g,ec}$ order of

Table 3. Electrochemical data and hole-carrier mobilities (μ) of **1**–**4**.

	E_{ox} [V]	HOMO [eV]	E_{red} [V]	LUMO [eV]	$E_{g,ec}$ [eV]	$E_{g,opt}$ [eV]	μ [cm^2 V^{-1} s^{-1}]
1	0.58	−5.31	−1.17	−3.56	1.75	2.08	5.08×10^{-5}
2	0.56	−5.29	−1.15	−3.58	1.71	2.07	2.04×10^{-4}
3	0.56	−5.29	−1.14	−3.59	1.70	2.06	1.46×10^{-4}
4	0.55	−5.28	−1.15	−3.58	1.70	2.05	5.79×10^{-5}

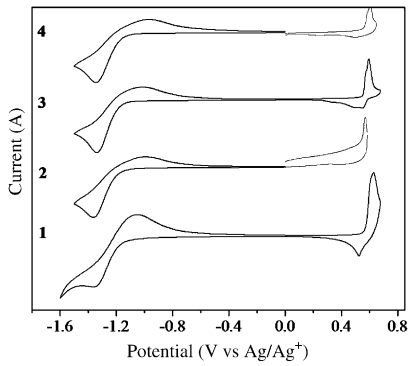

Figure 4. Cyclic voltammograms of **1**–**4** in acetonitrile containing 0.1 M $[Bu_4N][PF_6]$ at a scan rate of 50 mV s^{-1}.

1 (1.75 eV) > **2** (1.71 eV) > **3** (1.70 eV) ≈ **4** (1.70 eV) is consistent with the increasing length of π conjugation of **1**–**4**.

Table 4. Absorption transitions for **1**–**4** as calculated by the TD-DFT method.

	State	Transition	Contribution [%]	*E* [nm]	Oscillator strength	Measured value [nm]
1	S4	HOMO→LUMO	90	631	1.8807	514
		HOMO−1→LUMO+1	8			
	S5	HOMO→LUMO+1	64	564	0.2943	363
		HOMO−1→LUMO	34			
	S18	HOMO→LUMO+2	90	419	0.8826	307
2	S4	HOMO→LUMO	88	630	2.3648	506
		HOMO−1→LUMO+1	10			
	S17	HOMO→LUMO+2	92	442	1.0214	311
3	S4	HOMO→LUMO	84	635	2.6555	507
		HOMO−1→LUMO+1	12			
	S6	HOMO→LUMO+1	64	582	0.2605	439
		HOMO−1→LUMO	26			
	S16	HOMO→LUMO+2	92	467	1.0148	313
4	S5	HOMO→LUMO	80	630	3.1274	508
		HOMO−1→LUMO+1	16			
	S15	HOMO→LUMO+2	80	479	0.8222	461
		HOMO−2→LUMO+1	8			
	S16	HOMO−2→LUMO+1	62	478	0.1139	315
		HOMO−3→LUMO	12			
		HOMO−1→LUMO+2	10			

Computational Studies

Time-dependent density functional theory (TD-DFT) calculations were carried out for **1**–**4** to gain better insight into the electronic and spectroscopic properties as well as the nature of absorption bands for our new compounds. The DFT method at the gradient-corrected correlation functional level UPBE1PBE[26] was used to optimize the ground-state geometries of **1**–**4**. On the basis of the ground-state optimized geometry, 20 singlet excited states for **1**–**4** were calculated at the UPBE1PBE/6-31G (d, p) levels with the TD-DFT approach. As shown from the orbital profiles in Figure 5, the HOMO levels of **1**–**4** are mainly located at the π-conjugated thiophene ligands and the electron-donating triarylamine unit. The LUMOs of **1**–**4** have amplitudes mostly on the electron-accepting benzothiadiazole unit. As indicated in Table 4, the calculated lowest-energy absorption (from the HOMO→LUMO (84–90%) and HOMO−1→LUMO+1 (8–16%)) can be primarily assigned to the ICT transitions from the electron-donating thiophene and triarylamine groups to the electron-accepting benzothiadiazole unit. The absorption peaks were calculated at 419 nm for **1**, 442 nm for **2**, 467 nm for **3**, and 479 nm for **4** from the HOMO→LUMO+2 transitions, which arise from π→π* transitions of arylene ethynylene ligands, and they roughly follow the same trend as the experimentally measured absorption data (307 nm for **1**, 311 nm for **2**, 313 nm for **3**, and 315 nm for **4**). The main absorption energies for **1**–**4** from TD-DFT calculations suggest that addition of the triphenylamine and thiophene groups can increase the HOMO and HOMO−1 energy levels [HOMO: **1** (−5.01 eV) < **2** (−4.98 eV) < **3** (−4.96 eV) ≤ **4** (−4.96 eV); HOMO−1: **1** (−5.22 eV) < **2** (−5.18 eV) < **3** (−5.16 eV) < **4** (−5.13 eV)] by reducing the energy gaps for the HOMO/HOMO−1→LUMO+*n* transitions, leading to enhancement of the absorption ability of the corresponding compounds (Table 5).

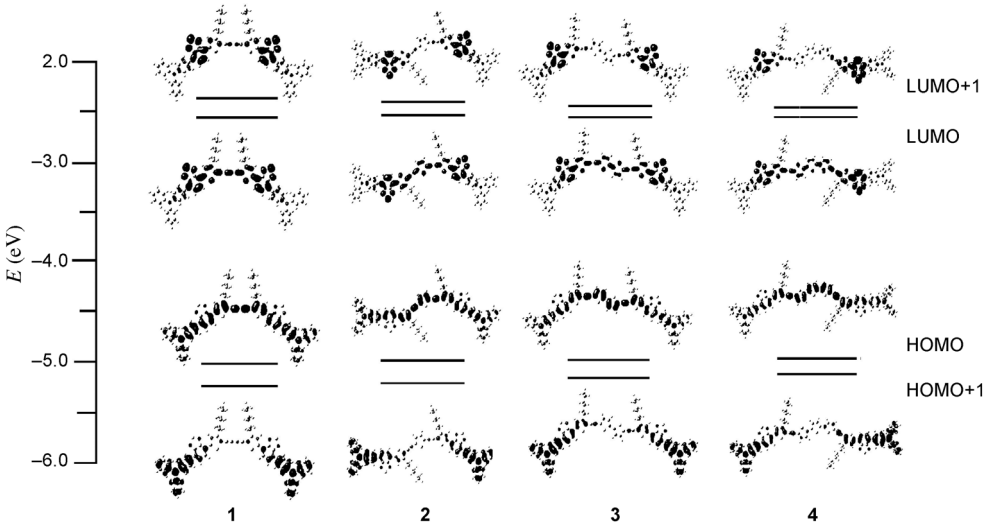

Figure 5. Contour plots of selected frontier molecular orbitals for **1**–**4**.

Table 5. Energy levels (in eV) of the frontier molecular orbitals for **1**–**4**.

	1	**2**	**3**	**4**
LUMO+1	−2.39	−2.41	−2.45	−2.46
LUMO	−2.59	−2.56	−2.56	−2.54
HOMO	−5.01	−4.98	−4.96	−4.96
HOMO−1	−5.22	−5.18	−5.16	−5.13

Performance of Organic Solar Cells

To demonstrate the potential of **1**–**4** as electron-donor materials in photovoltaic applications, BHJ devices were fabricated using $PC_{70}BM$ as the acceptor. The hole-collection electrode consisted of indium tin oxide (ITO) with a spin-coated poly(3,4-ethylenedioxythiophene)/poly(styrene sulfonate) (PEDOT/PSS) layer, whereas Al served as the electron-collecting electrode. The active layers were prepared by spin-coating a solution of **1**–**4** with $PC_{70}BM$ in 1:3 (w/w) ratio in chlorobenzene. The photovoltaic data were collected under simulated AM 1.5G solar illumination at the irradiation intensity of 100 mW cm^{-2}. As a very thick active layer can slow down the charge transport and a very thin one can reduce the absorption of the irradiated light, active layers with different thickness were measured. The results are summarized in Table 6. The optimal thickness of the active layer was found to be 60, 65, 80, and 60 nm for **1**–**4**, respectively.

The current density versus voltage (*J*–*V*) curves of the BHJ devices based on **1**–**4**:$PC_{70}BM$ (1:3, w/w) blends with different active layer thickness are plotted in Figure 6. The devices based on **4**, which possesses the longest π-conjugated framework, showed the highest PCE (3.68%) among all the devices, with high V_{oc} of 0.96 V, short-circuit photocurrent density (J_{sc}) of 8.08 mA cm^{-2}, and fill factor (FF) of 0.48 at the optimized active layer thickness of 60 nm, which indicates that the photovoltaic performance can be significantly improved by introducing a long π-conjugated chain or a strong D group in the molecule. The device based on **1**, which lacks a thiophene donor within the molecule, still showed a PCE of 3.11% with attractive V_{oc} of 0.97 V, J_{sc} of 7.85 mA cm^{-2}, and FF of 0.41. These results suggest that these kinds of conjugated oligothiophene-bridged bis(arylene ethynylene) molecules are promising materials for BHJ solar cell applications. Moreover, more work needs to be carried out in the future to establish the exact structure–property correlations (e.g. dependence of the device performance and other parameters on the number of thiophene rings) of these materials.

Table 6. OSC device performance based on **1**–**4**:$PC_{70}BM$ blends (1:3, w/w).

Donor	Film thickness [nm]	V_{oc} [V]	J_{sc} [mA cm^{-2}]	FF	PCE [%]
1	60	0.97	7.85	0.41	3.11
	75	0.96	6.91	0.42	2.80
2	65	0.91	7.96	0.44	3.19
	85	0.90	7.26	0.42	2.77
3	60	0.93	7.03	0.44	2.86
	80	0.94	7.75	0.42	3.07
4	60	0.96	8.08	0.48	3.68
	75	0.95	7.76	0.44	3.28

The charge-carrier mobility is one of the important factors that affect the J_{sc} of BHJ devices. A high hole mobility of the electron donor allows effective charge carrier transport to the electrodes and reduces the photocurrent loss by recombination. The hole mobilities of **1**–**4** were examined using organic field-effect transistors (OFETs), and the results revealed that typical p-type characteristics were observed for **1**–**4** with good charge-transporting properties. The hole mobilities were found to be 5.08×10^{-5}, 2.04×10^{-4}, 1.46×10^{-4}, and 5.79×10^{-5} cm^2 V^{-1} s^{-1} for **1**–**4**, respectively (Table 3). In addition, the mobility of the active material

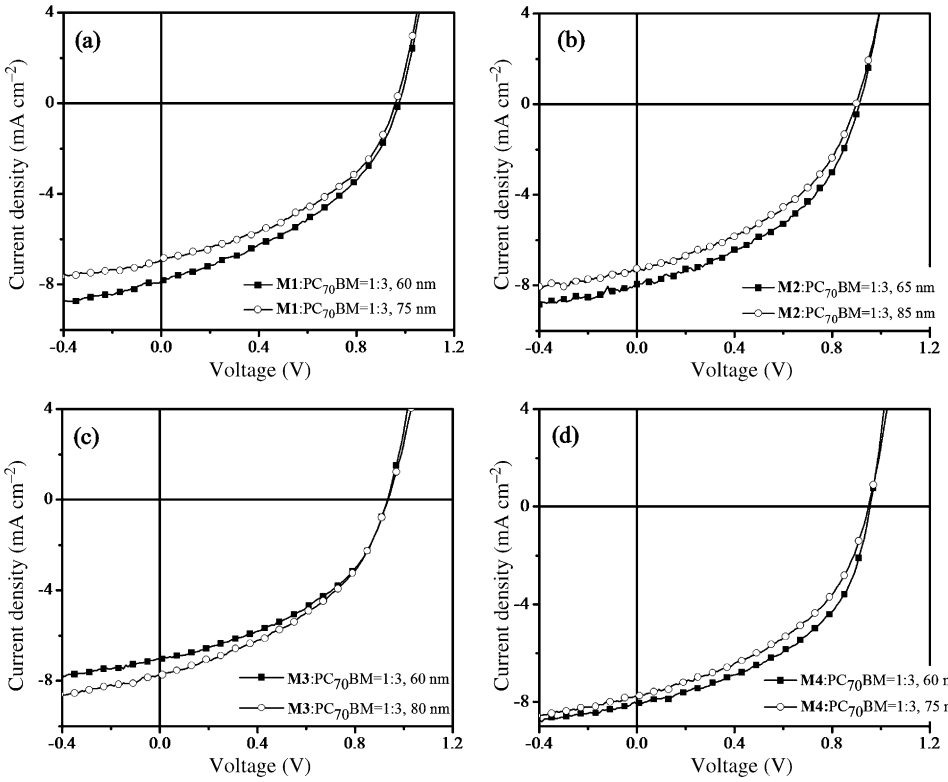

Figure 6. Current density–voltage (*J*–*V*) curves of OSCs based on a) **1**, b) **2**, c) **3**, and d) **4** with different active layer thickness under illumination of AM 1.5G at 100 mW cm^{-2}.

was also shown to exert a great influence on the FF of the photovoltaic device.[27] The FF values of the photovoltaic devices based on **1–4** are not very impressive, partly due to the relatively low hole mobilities of **1–4** and their poor charge mobility balance.

To push the PCE of OSCs towards the predicted theoretical limit,[28] achieving high values in both J_{sc} and V_{oc} is critical. The devices based on **1–4** exhibited very high V_{oc} of over 0.9 V in each case, regardless of the oligothienyl chain length. This result is in line with their HOMOs being localized on the same core unit.[29] The highest V_{oc} of 0.97 V was obtained in **1** with an active layer thickness of 60 nm. Therefore, our system can narrow the bandgap of the molecules without sacrificing efficient charge separation and high V_{oc} value, and we can thus tackle the major hurdle in achieving high efficiency in traditional OSCs. The performance of these devices was also supported by the results for the external quantum efficiency (EQE) characteristics (Figure 7). The monochromatic spectrum presents a broad and strong response spanning from 350 to 720 nm, with the maximum EQE values of 51, 56, 56, and 57% at 503, 460, 485, and 476 nm for **1–4**, respectively.

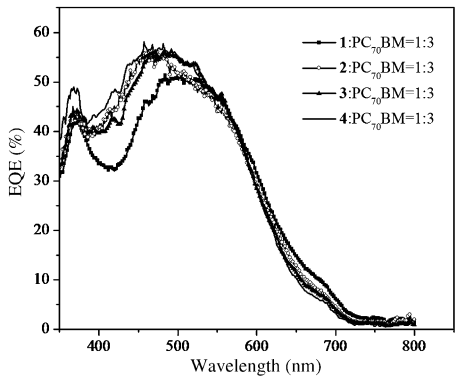

Figure 7. External quantum efficiency (EQE) spectra of **1–4**.

Conclusions

A new series of oligothiophene-spaced bis(arylene ethynylene) compounds **1–4** were obtained by convenient synthetic processes. The optical, electronic, and electrochemical properties of **1–4** have been investigated. As demonstrated by the optical studies, the absorption features of these oligomers are significantly broadened by the D-A-spacer-A-D motif, hence enhancing the overlap of the absorption of **1–4** with the solar spectrum. The TD-DFT calculations showed that the HOMOs are mainly located at the central π-conjugated ligands and the electron-donating triarylamine group, while the LUMOs of **1–4** have amplitudes mostly on the electron-accepting benzothiadiazole unit. In addition, the computational data show that the lowest-energy absorption can be primarily assigned to the ICT transitions from the electron-donating thiophene and triarylamine groups to the electron-accepting benzothiadiazole unit, suggesting that addition of the triarylamine and thiophene groups can lead to the enhancement of the absorption ability of these compounds by reducing the energy gaps of the HOMO/HOMO−1→LUMO+n transitions. By increasing the oligothiophene chain length, we achieved the highest PCE value of 3.68% using a solar cell based on compound **4**. All of the devices based on **1–4** exhibited high V_{oc} values (>0.90 V) due to their optimal HOMO and LUMO levels. Hence, bis(arylene ethynylene) compounds of this kind with good solution processibility are promising materials for application in BHJ solar cells, and this demonstration will stimulate more work on the development of these small organic molecules for photovoltaic applications. Further improvement in the device efficiency can be achieved by tuning the ICT absorption and energy levels of this type of materials as well as their oligomeric chain length and thin film morphology.

Experimental Section

Materials and Reagents

All of the manipulations were performed under a dry nitrogen atmosphere by using Schlenk techniques. Solvents were dried by standard methods and distilled prior to use except for those of spectroscopic grade for the photophysical and electrochemical measurements.

Physical Measurements

Infrared spectra were recorded on a Nicolet Magna 550 Series II FT-IR spectrometer using KBr pellets for solid-state spectroscopy. NMR spectra were measured on deuterated solvents as the lock and reference on a Bruker AV 400 instrument with ^{1}H and ^{13}C NMR chemical shifts quoted relative to tetramethylsilane standard. The matrix-assisted laser desorption ionization time-of-flight (MALDI-TOF) mass spectra were recorded on a Autoflex Bruker MALDI-TOF system. UV/Vis absorption spectra were obtained on an HP-8453 diode array spectrophotometer. The photoluminescence spectra were measured in dichloromethane with a PTI Fluorescence Master Series QM1 spectrophotometer. Cyclic voltammograms were measured on a CHI model 600D electrochemistry station in 0.1 mol L^{-1} $[Bu_4N][PF_6]$ in acetonitrile with a glassy carbon working electrode, a Pt wire counter electrode, and a Ag/AgCl reference electrode under a N_2 atmosphere at a scan rate of 50 mV s^{-1}.

DFT and TD-DFT Computational Methods

The DFT method at the gradient-corrected correlation functional level UPBE1PBE was used to optimize the ground state geometries of **1–4**. On the basis of the ground-state optimized geometry, 20 singlet excited states for **1–4** were calculated to determine the vertical excitation energies using the TD-DFT method at the UPBE1PBE level. The 6-31G (d, p) effective core potential basis set was applied for all atoms. All calculations were performed using the Gaussian 03 program package.[30]

Fabrication and Characterization of Organic Field-Effect Transistors (OFETs)

Silicon wafers (n-type) with a thermal oxide layer (300 nm) were used as substrates. Films of 5 nm chromium (as an adhesion layer) and 40 nm gold were evaporated on the surface of SiO_2 through a shadow mask as source and drain electrodes. The channel width (W) and length (L) were 2.0 mm and 0.1 mm, respectively. Organic semiconductors were dissolved in toluene with a concentration of 10 mg mL^{-1}. The solutions were stirred for 12 h at 60 °C and then spin-coated onto the substrates, followed by thermal annealing (60 °C) process in a glove box filled with high-purity nitrogen. The OFETs were characterized in the glove box with a semiconductor parameter analyzer (Agilent 4156C). For transfer characteristics (I_D–V_G), the channel current I_D between source and drain was measured

as a function of gate voltage V_G under a constant drain voltage. For output characteristics (I_D–V_{DS}), the channel current I_D was measured as a function of drain voltage V_{DS} under a constant gate voltage V_G, and different V_G values resulted in different curves of I_D versus V_{DS}. The field effect mobility of each transistor was calculated in the saturation regime ($V_{DS} = -100$ V) by plotting the square root of channel current I_D versus gate voltage V_G and fitting the curve by Equation (1):

$$\mu = \frac{2L}{WC_i}\left(\frac{d\sqrt{I_D}}{dV_G}\right)^2 \quad (1)$$

where C_i is the capacitance of the gate oxide with an unit area.

Fabrication and Characterization of Bulk Heterojunction Solar Cells

A BHJ device configuration of ITO/PEDOT:PSS/active layer/LiF/Al was used, in which the active layer consisted of a blend film of **1**–**4** as the electron donor and $PC_{70}BM$ as the electron acceptor in a weight ratio of 1:3. ITO glass substrates (10 Ω per square) were cleaned by sonication in toluene, acetone, ethanol, and deionized water in sequence; dried in an oven; and then cleaned with UV ozone for 300 s. PEDOT:PSS (Baytron P AI 4083) was spin-coated onto the cleaned ITO substrate to form a 40 nm thick layer, followed by drying at 120 °C for 30 min in air. Then, the substrates were transferred to a glove box filled with nitrogen. A prepared solution containing a mixture of **1**–**4**:$PC_{70}BM$ (1:3, w/w) in chlorobenzene was spin-coated on top of the PEDOT:PSS layer. Finally, the samples were transferred into an evaporator where 1 nm of LiF and 80 nm of Al were thermally deposited under vacuum at 10^{-6} Torr. The devices were encapsulated in the glove box and measured in air. Current–voltage characteristics were measured using a computer-controlled Keithley 236 source meter. The photocurrent was measured under AM 1.5G illumination at 100 mW cm^{-2} from a solar simulator (Oriel, 91160 A-1000). The EQE spectrum was measured at a chopping frequency of 275 Hz with a lock-in amplifier (Stanford, SR830) during illumination with the monochromatic light from a xenon lamp. The AFM measurements were performed on a SPA300HV instrument with an SPI3800 controller (Seiko Instruments). The images were taken with the tapping mode.

*Synthesis of **1**–**4***

The compounds thiophen-2-ylboronic acid, 4-bromo-7-(4-hexyl-2-thienyl)-2,1,3-benzothiadiazole and 4-(*N*,*N*-di-*p*-tolyl-4-aminophenyl)-7-(4-hexyl-5-ethynyl-2-thienyl)-2,1,3-benzothiadiazole (**L1**) were prepared according to the literature methods.[17] 2,5′-Diiodo-2,2′-bithiophene[31] and 5,5″-diiodo-2,2′:5′,2″-terthiophene[32] were prepared as published. Other chemicals were commercially available and used as received unless otherwise stated.

Compound **1**: Under a N_2 atmosphere, ligand **L1** (0.2 g, 0.388 mmol) was added to a mixture of $[Pd(PPh_3)_4]$ (22.4 mg, 0.019 mmol) and CuI (5.5 mg, 0.029 mmol) in NEt_3 and $CHCl_3$ (1:1, v/v, 16 mL). The reaction mixture was stirred at room temperature overnight. The solvent was then removed under reduced pressure to obtain the crude product, which was purified by chromatography over a silica column using *n*-hexane/CH_2Cl_2 (1:1, v/v) as eluent to afford a pure sample of **1** as a dark red solid in very high yield (193.5 mg, yield: 97%). ^{1}H NMR ($CDCl_3$, 400 MHz): δ = 7.93 (m, 2H, Ar), 7.90–7.88 (m, 2H, Ar), 7.85–7.83 (m, 4H, Ar), 7.69–7.68 (m, 2H, Ar), 7.15–7.07 (m, 20H, Ar), 2.85–2.81 (t, J = 7.6 Hz, 4H, alkyl), 2.33 (s, 12H, CH_3), 1.77–1.74 (m, 4H, alkyl), 1.45–1.35 (m, 12H, alkyl), 0.94–0.88 ppm (m, 6H, alkyl); ^{13}C NMR (100 MHz, $CDCl_3$): δ = 153.89, 152.73, 151.95, 148.64, 144.83, 140.91, 133.19, 130.01, 129.79, 129.42, 128.23, 126.78, 126.23, 125.24, 124.59, 123.54, 121.42, 118.25 (Ar), 81.85, 77.98 (C≡C), 53.43, 31.59, 30.33, 28.98, 22.66, 20.88, 14.13 ppm (alkyl); IR (KBr): $\tilde{\nu}$ = 2124 cm^{-1} (w, ν(C≡C)); MALDI-TOF-MS (*m/z*): 1191.4 $[M]^+$. Elemental anal. (%) calcd for $C_{76}H_{68}N_6S_4$: C 76.47, H 5.74, N 7.04; found: C 76.65, H 5.89, N 7.11.

General procedure for the synthesis of the oligothiophene-bridged bis(arylene ethynylene) compounds **2**–**4**: These compounds were prepared by the Sonogashira coupling reaction between **L1** and the corresponding diiodo-substituted oligothiophene precursors using the $Pd(OAc)_2$/CuI/PPh_3 catalyst system. Under a N_2 atmosphere, $Pd(OAc)_2$ (3 mol%), CuI (5 mol%), and PPh_3 (9 mol%) were added to an ice-cooled mixture of each appropriate diiodo-substituted oligothiophene in CH_2Cl_2/NEt_3 (v/v, 1:1) solution. After the solution was stirred for 30 min at 0 °C, ligand **L1** (2.1 equiv) was then added and the suspension was stirred for another 30 min at the same temperature before being warmed to room temperature. After reacting for another 30 min at room temperature, the mixture was heated to 52 °C overnight. Then, the solution was cooled to room temperature and the solvent mixture was evaporated under reduced pressure. The crude product was purified by column chromatography on silica gel with a solvent combination of CH_2Cl_2/*n*-hexane (1:2, v/v) as eluent to give pure products of **2**–**4** in good yields (62–69%).

Compound **2**: Yield: 69%, dark red solid. ^{1}H NMR (400 MHz, $CDCl_3$): δ = 7.93 (m, 2H, Ar), 7.90–7.87 (d, J = 7.6 Hz, 2H, Ar), 7.85–7.83 (m, 4H, Ar), 7.68–7.66 (d, J = 7.6 Hz, 2H, Ar), 7.15–7.07 (m, 22H, Ar), 2.84–2.80 (t, J = 7.6 Hz, 4H, alkyl), 2.33 (s, 12H, CH_3), 1.79–1.72 (m, 4H, alkyl), 1.45–1.35 (m, 10H, alkyl), 0.93–0.88 ppm (m, 8H, alkyl); ^{13}C NMR (100 MHz, $CDCl_3$,): δ = 153.92, 152.74, 149.47, 148.60, 144.87, 140.16, 137.22, 133.16, 132.98, 134.69, 130.01, 129.78, 129.50, 128.29, 126.83, 125.97, 125.23, 124.77, 121.46, 118.69 (Ar), 89.71, 87.83 (C≡C), 31.65, 30.26, 29.91, 29.70, 29.00, 22.64, 14.14 ppm (alkyl); IR (KBr): $\tilde{\nu}$ = 2057 cm^{-1} (w, ν(C≡C)); MALDI-TOF-MS (*m/z*): 1274.4 $[M]^+$. Elemental anal. (%) calcd for $C_{80}H_{70}N_6S_5$: C 75.32, H 5.53, N 6.59; found: C 75.43, H 5.76, N 6.82.

Compound **3**: Yield: 62%, dark red solid. ^{1}H NMR (400 MHz, $CDCl_3$): δ = 7.94 (s, 2H, Ar), 7.91–7.89 (d, J = 7.6 Hz, 2H, Ar), 7.85–7.83 (m, 4H, Ar), 7.69–7.67 (d, J = 7.6 Hz, 2H, Ar), 7.19–7.18 (d, J = 3.6 Hz, 2H, Ar), 7.15–7.14 (m, 2H, Ar), 7.13–7.07 (m, 20H, Ar), 2.84–2.80 (t, J = 7.6 Hz, 4H, alkyl), 2.34 (s, 12H, CH_3), 1.78–1.74 (m, 4H, alkyl), 1.37–1.25 (m, 12H, alkyl), 0.93–0.88 ppm (m, 6H, alkyl); ^{13}C NMR (100 MHz, $CDCl_3$): δ = 153.88, 152.71, 149.22, 148.55, 144.85, 140.00, 138.22, 133.12, 132.86, 132.64, 129.99, 129.76, 129.50, 128.27, 126.79, 125.88, 125.21, 124.75, 124.09, 122.57, 121.50, 118.82 (Ar), 89.92, 88.11 (C≡C), 31.65, 30.25, 29.89, 29.69, 29.00, 22.65, 14.16 ppm (alkyl); IR (KBr): 2058 cm^{-1} (w, ν-(C≡C)); MALDI-TOF-MS (*m/z*): 1357.3 $[M]^+$. Elemental anal. (%) calcd for $C_{84}H_{72}N_6S_6$: C 74.30, H 5.34, N 6.19; found: C 74.53, H 5.39, N 6.38.

Compound **4**: Yield: 64%, dark red solid. ^{1}H NMR (400 MHz, $CDCl_3$): δ = 7.93 (m, 2H, Ar), 7.90–7.80 (d, J = 7.6 Hz, 2H, Ar), 7.85–7.83 (m, 4H, Ar), 7.68–7.67 (d, J = 7.6 Hz, 2H, Ar), 7.19–7.18 (d, J = 4.0 Hz, 2H, Ar), 7.15–7.07 (m, 24H, Ar), 2.83–2.80 (t, J = 7.6 Hz, 4H, alkyl), 2.34 (s, 12H, CH_3), 1.77–1.72 (m, 4H, alkyl), 1.43–1.25 (m, 8H, alkyl), 0.93–0.87 ppm (m, 10H, alkyl); ^{13}C NMR (100 MHz, $CDCl_3$): δ = 153.93, 152.75, 149.22, 148.59, 144.86, 139.98, 138.47, 131.11, 133.16, 132.93, 132.68, 130.00, 129.78, 129.52, 188.31, 126.85, 125.94, 125.22, 124.95, 124.82, 123.79, 122.26, 121.47, 118.88 (Ar), 89.96, 88.00 (C≡C), 31.66, 30.27, 29.00, 22.66, 20.88, 14.16, 14.13 ppm (alkyl); IR (cm^{-1}): $\tilde{\nu}$ = 2058 cm^{-1} (w, ν(C≡C)); MALDI-TOF-MS (*m/z*): 1438.9 $[M]^+$. Elemental anal. (%) calcd for $C_{88}H_{74}N_6S_7$: C 73.40, H 5.18, N 5.84; found: C 73.55, H 5.36, N 5.98.

Acknowledgements

We thank Hong Kong Baptist University (FRG2/12-13/083), Hong Kong Research Grants Council (HKBU203011) and Areas of Excellence Scheme, University Grants Committee of HKSAR (project No. [AoE/P-03/08]) and the National Natural Science Foundation of China (project number 21029001) for financial support. The work described in this paper was also partially supported by a grant from the Research Grants Council of the Hong Kong Special Administrative Region, China (Project No. [T23-713/11]).

[1] a) S. C. Roy, O. K. Varghese, M. Paulose, C. A. Grimes, *ACS Nano* **2010**, *4*, 1259–1278; b) J. A. Turner, *Science* **1999**, *285*, 687–689; c) R. Eisenberg, D. G. Nocera, *Inorg. Chem.* **2005**, *44*, 6799–6801.

[2] a) W. Würfel, *Physics of Solar Cells*, Wiley-VCH, Weinheim, **2005**; b) X. H. Wang, G. I. Koleilat, J. Tang, H. Liu, I. J. Kramer, *Nat. Photonics* **2011**, *5*, 480–484; c) C. H. Chou, L. K. Wei, Z. Hong, L. M. Chen, Y. Yang, *Adv. Mater.* **2011**, *23*, 1282–1286.
[3] a) Y. J. Cheng, S. H. Yang, C. S. Hsu, *Chem. Rev.* **2009**, *109*, 5868–5923; b) P. T. Boudreault, A. Najari, M. Leclerc, *Chem. Mater.* **2011**, *23*, 456–469; c) Y. F. Li, *Acc. Chem. Res.* **2012**, *45*, 723–733.
[4] a) J. Peet, M. L. Senatore, A. J. Heeger, G. C. Bazan, *Adv. Mater.* **2009**, *21*, 1521–1527; b) B. C. Thompson, J. M. J. Fréchet, *Angew. Chem.* **2008**, *120*, 62–82; *Angew. Chem. Int. Ed.* **2008**, *47*, 58–77; c) S. Günes, H. Neugebauer, N. S. Sariciftci, *Chem. Rev.* **2007**, *107*, 1324–1338.
[5] J. Peet, J. Y. Kim, N. E. Coates, W. L. Ma, D. Moses, A. J. Heeger, G. C. Bazan, *Nat. Mater.* **2007**, *6*, 497–500.
[6] a) Y. Lin, Y. Li, X. Zhan, *Chem. Soc. Rev.* **2012**, *41*, 4245–4272; b) F. Silvestri, M. D. Irwin, L. Beverina, A. Facchetti, G. A. Pagani, T. J. Marks, *J. Am. Chem. Soc.* **2008**, *130*, 17640–17641; c) R. Koeppe, N. S. Sariciftci, P. A. Troshin, R. N. Lyubovskaya, *Appl. Phys. Lett.* **2005**, *87*, 244102.
[7] Z. He, C. Zhong, X. Huang, W.-Y. Wong, H. Wu, L. Chen, S. Su, Y. Cao, *Adv. Mater.* **2011**, *23*, 4636–4643.
[8] Z. C. He, C M. Zhong, S. J. Su, M. Xu, H. B. Wu, Y. Cao, *Nat. Photonics* **2012**, *6*, 591–595.
[9] a) O. Hagemann, M. Jorgensen, F. C. Krebs, *J. Org. Chem.* **2006**, *71*, 5546–5559; b) L. Schmidt-Mende, A. Fechtenkotter, K. Mullen, E. Moons, R. H. Friend, J. D. MacKenzie, *Science* **2001**, *293*, 1119–1122; c) S. Roquet, A. Cravino, P. Leriche, O. Aleveque, P. Frere, J. Roncali, *J. Am. Chem. Soc.* **2006**, *128*, 3459–3466; d) C. Q. Ma, M. Fonrodona, M. C. Schikora, M. M. Wienk, R. A. J. Janssen, P. Bauerle, *Adv. Funct. Mater.* **2008**, *18*, 3323–3331; e) M. T. Lloyd, A. C. Mayer, S. Subramanian, D. A. Mourey, D. J. Herman, A. V. Bapat, J. E. Anthony, G. G. Malliaras, *J. Am. Chem. Soc.* **2007**, *129*, 9144–9149; f) C. H. Huang, N. D. McClenaghan, A. Kuhn, J. W. Hofstraat, D. M. Bassani, *Org. Lett.* **2005**, *7*, 3409–3412; g) A. B. Tamayo, X. D. Dang, B. Walker, J. Seo, T. Kent, T. Q. Nguyen, *Appl. Phys. Lett.* **2009**, *94*, 103301; h) A. B. Tamayo, B. Walker, T. Q. Nguyen, *J. Phys. Chem. C* **2008**, *112*, 11545–11551.
[10] a) M. M. Wienk, J. M. Kroon, W. J. H. Verhees, J. Knol, J. C. Hummelen, *Angew. Chem.* **2003**, *115*, 3493–3497; b) J. W. Arbogast, C. S. Foote, *J. Am. Chem. Soc.* **1991**, *113*, 8886–8889.
[11] a) J. Roncali, *Acc. Chem. Res.* **2009**, *42*, 1719–1730; b) B. Walker, C. Kim, T. Q. Nguyen, *Chem. Mater.* **2011**, *23*, 470–482; c) J. Zhang, D. Deng, C. He, Y. He, M. Zhang, Z. G. Zhang, Z. Zhang, Y. Li, *Chem. Mater.* **2011**, *23*, 817–822.
[12] I. N. Hulea, S. Fratini, H. Xie, C. L. Mulder, N. N. Iossad, G. Rastelli, S. Ciuchi, A. F. Morpurgo, *Nat. Mater.* **2006**, *5*, 982–986.
[13] Y. Li, Q. Guo, Z. Li, J. Pei, W. Tian, *Energy Environ. Sci.* **2010**, *3*, 1427–1436.
[14] a) C. J. Takacs, Y. Sun, G. C. Welch, L. A. Perez, X. Liu, W. Wen, G. C. Bazan, A. J. Heeger, *J. Am. Chem. Soc.* **2012**, *134*, 16597–16606; b) Y. J. Cheng, C. H. Hsieh, Y. J. He, C. S. Hsu, Y. F. Li, *J. Am. Chem. Soc.* **2010**, *132*, 17381–17383.
[15] a) J. Song, F. Zhang, C. Li, W. Liu, B. Li, Y. Huang, Z. Bo, *J. Phys. Chem. C* **2009**, *113*, 13391–13397; b) C.-P. Hsieh, H.-P. Lu, C.-L. Chiu, C.-W. Lee, S.-H. Chuang, C.-L. Mai, W.-N. Yen, S.-J. Hsu, E. W.-G. Diau, C.-Y. Yeh, *J. Mater. Chem.* **2010**, *20*, 1127–1134; c) W.-Y. Wong, C.-L. Ho, *Acc. Chem. Res.* **2010**, *43*, 1246–1256.
[16] C. J. Brabec, A. Cravino, D. Meissner, N. S. Sariciftci, T. Fromherz, M. T. Rispens, L. Sanchez, J. C. Hummelen, *Adv. Funct. Mater.* **2001**, *11*, 374–380.
[17] F. R. Dai, H. M. Zhan, Q. Liu, Y. Y. Fu, J. H. Li, Q. W. Wang, Z. Y. Xie, L. X. Wang, F. Yan, W.-Y. Wong, *Chem. Eur. J.* **2012**, *18*, 1502–1511.
[18] S. Takahashi, Y. Kuroyama, K. Sonogashira, N. Hagihara, *Synthesis* **1980**, 627–630.
[19] a) P. M. Beaujuge, H. N. Tsao, M. R. Hansen, C. M. Amb, J. R. Reynolds, *J. Am. Chem. Soc.* **2012**, *134*, 8944–8957; b) Q. J. Sun, H. Q. Wang, C. H. Yang, Y. F. Li, *J. Mater. Chem.* **2003**, *13*, 800–806; c) J. H. Hou, Z. A. Tan, Y. Yan, Y. J. He, C. H. Yang, Y. F. Li, *J. Am. Chem. Soc.* **2006**, *128*, 4911–4916.
[20] D. Magde, G. Rojas, P. G. Seybold, *Photochem. Photobiol.* **1999**, *70*, 737–744.
[21] J. Brédas, J. E. Norton, J. Cornil, V. Coropceanu, *Acc. Chem. Res.* **2009**, *42*, 1691–1699.
[22] Y. J. He, G. J. Zhao, B. Peng, Y. F. Li, *Adv. Funct. Mater.* **2010**, *20*, 3383–3389.
[23] a) J. M. Halls, J. Cornill, D. A. dos Santos, R. Silbey, D.-H. Hwang, A. B. Holmes, J. L. Brédas, R. H. Friend, *Phys. Rev. B* **1999**, *60*, 5721–5727; b) C. J. Brabec, C. Winder, N. S. Sariciftci, J. C. Hummelen, A. Dhanabalan, P. A. van Hal, R. A. J. Janssen, *Adv. Funct. Mater.* **2002**, *12*, 709–712.
[24] a) J. H. Hou, H. Y. Chen, S. Q. Zhang, G. Li, Y. Yang, *J. Am. Chem. Soc.* **2008**, *130*, 16144–16145; b) H. Y. Chen, J. H. Hou, S. Q. Zhang, Y. Y. Liang, G. W. Yang, Y. Yang, L. P. Yu, Y. Wu, G. Li, *Nat. Photonics* **2009**, *3*, 649–653.
[25] L. J. A. Koster, V. D. Mihailetchi, R. Ramaker, P. W. M. Blom, *Appl. Phys. Lett.* **2005**, *86*, 123509.
[26] J. P. Perdew, K. Burke, M. Ernzerhof, *Phys. Rev. Lett.* **1996**, *77*, 3865–3868.
[27] J. K. J. van Duren, X. Yang, J. Loos, C. W. T. Bulle-Lieuwma, A. B. Sieval, J. C. Hummelen, R. A. J. Janssen, *Adv. Funct. Mater.* **2004**, *14*, 425–434.
[28] M. C. Scharber, D. Mühlbacher, M. Koppe, P. Denk, C. Waldauf, A. J. Heeger, C. J. Brabec, *Adv. Mater.* **2006**, *18*, 789–794.
[29] X. Y. Zhao, C. Piliego, B. Kim, D. A. Poulsen, B. Ma, D. A. Unruh, J. M. J. Fréchet, *Chem. Mater.* **2010**, *22*, 2325–2332.
[30] Gaussian 03 (Revision B), M. J. Frisch, G. W. Trucks, H. B. Schlegel, G. E. Scuseria, M. A. Robb, J. R. Cheeseman, J. A. Montgomery, Jr., T. Vreven, K. N. Kudin, J. C. Burant, J. M. Millam, S. S. Iyengar, J. Tomasi, V. Barone, B. Mennucci, M. Cossi, G. Scalmani, N. Rega, G. A. Petersson, H. Nakatsuji, M. Hada, M. Ehara, K. Toyota, R. Fukuda, J. Hasegawa, M. Ishida, T. Nakajima, Y. Honda, O. Kitao, H. Nakai, M. Klene, X. Li, J. E. Knox, H. P. Hratchian, J. B. Cross, V. Bakken, C. Adamo, J. Jaramillo, R. Gomperts, R. E. Stratmann, O. Yazyev, A. J. Austin, R. Cammi, C. Pomelli, J. W. Ochterski, P. Y. Ayala, K. Morokuma, G. A. Voth, P. Salvador, J. J. Dannenberg, V. G. Zakrzewski, S. Dapprich, A. D. Daniels, M. C. Strain, O. Farkas, D. K. Malick, A. D. Rabuck, K. Raghavachari, J. B. Foresman, J. V. Ortiz, Q. Cui, A. G. Baboul, S. Clifford, J. Cioslowski, B. B. Stefanov, G. Liu, A. Liashenko, P. Piskorz, I. Komaromi, R. L. Martin, D. J. Fox, T. Keith, M. A. Al-Laham, C. Y. Peng, A. Nanayakkara, M. Challacombe, P. M. W. Gill, B. Johnson, W. Chen, M. W. Wong, C. Gonzalez, J. A. Pople, Gaussian, Inc., Pittsburgh, PA, **2003**.
[31] G. Sotgiu, M. Zambianchi, G. Barbarella, C. Botta, *Tetrahedron* **2002**, *58*, 2245–2251.
[32] M. Melucci, G. Barbarella, M. Zambianchi, P. Di Pietro, A. Bongini, *J. Org. Chem.* **2004**, *69*, 4821–4828.

Received: March 25, 2013
Published online: May 6, 2013